Immunity
Article

How Punctual Ablation of Regulatory T Cells Unleashes an Autoimmune Lesion within the Pancreatic Islets

Markus Feuerer,[1,2] Yuelei Shen,[4,5] Dan R. Littman,[4,5] Christophe Benoist,[1,2,*] and Diane Mathis[1,2,3,*]
[1]Department of Pathology
[2]Section on Immunology and Immunogenetics, Joslin Diabetes Center
[3]Harvard Stem Cell Institute
Harvard Medical School, Boston, MA 02115, USA
[4]The Kimmel Center for Biology and Medicine of the Skirball Institute
[5]Howard Hughes Medical Institute
New York University School of Medicine, New York, NY 10016, USA
*Correspondence: cbdm@hms.harvard.edu (C.B.), cbdm@hms.harvard.edu (D.M.)
DOI 10.1016/j.immuni.2009.08.023

SUMMARY

CD4$^+$Foxp3$^+$ regulatory T cells (Treg cells) are known to control the progression of autoimmune diabetes, but when, where, and how they exert their influence in this context are questions still under vigorous debate. Exploiting a transgene encoding the human diphtheria toxin receptor, we punctually and specifically ablated Foxp3$^+$ cells in the BCD2.5/NOD mouse model of autoimmune diabetes. Strikingly, overt disease developed within 3 days. The earliest detectable event was the activation of natural killer (NK) cells directly within the insulitic lesion, particularly the induction of *Ifng* gene expression within 7 hours of Treg cell ablation. Interferon-γ had a strong impact on the gene-expression program of the local CD4$^+$ T effector cell population, unleashing it to aggressively attack the islets, which was required for the development of diabetes. Thus, Treg cells regulate pancreatic autoimmunity in situ through control of a central innate immune system player, NK cells.

INTRODUCTION

Foxp3$^+$CD4$^+$ regulatory T (Treg) cells regulate a variety of immune responses, including autoimmunity, allergy, inflammation, infection, and tumorigenesis (Zheng and Rudensky, 2007; Sakaguchi et al., 2008). This cell population is required life-long to guard against autoimmunity, perhaps best illustrated by the multiorgan infiltrates that arise a few weeks after its acute ablation in adult mice (Kim et al., 2007). In particular, Treg cells play a crucial role in protection from type-1 diabetes (T1D), an autoimmune disease characterized by specific attack of the insulin-producing β cells of the pancreatic islets (Tang and Bluestone, 2008). For example, autoimmune diabetes is one of the major elements of the IPEX (immune dysfunction, polyendocrinopathy, entreropathy, X-linked inheritance) syndrome that afflicts humans with a defective Treg cell compartment due to a mutation in the *FOXP3* gene (Bennett et al., 2001; Wildin et al., 2001). Moreover, transfer of Treg cells can protect mice from autoimmune diabetes, whether in the NOD model or in T cell receptor (TCR) transgenic systems derived thereof (Salomon et al., 2000; Tarbell et al., 2004; Tang et al., 2004; Herman et al., 2004; Tarbell et al., 2007). Conversely, genetic deficiencies or experimental manipulations that reduce numbers or activity of this regulatory population can exacerbate diabetes (Salomon et al., 2000; Chen et al., 2005).

The precise point at which Treg cells impact on the behavior of effector T (Teff) cells to rein in autoimmunity, and the pathways involved, remain controversial issues (Zheng and Rudensky, 2007; Sakaguchi et al., 2008). Several junctures are possible and have been highlighted in different experimental settings: the migration of naive T cells to the lymph nodes (LNs) draining the target tissue(s); their activation, expansion, or survival therein; differentiation to a particular T helper (Th) cell phenotype; homing of activated Teff cells to target tissues; their expansion or survival after arrival; and their ultimate destructiveness toward the tissues.

Concerning diabetes, several groups have focused on Treg cell influences at an early stage—initial priming of potentially diabetogenic T cells within the pancreatic LNs (PLNs). Proliferation of islet-reactive BDC2.5 Teff cells in the PLNs was inhibited by preadministration of a large number of Treg cells and, conversely, was enhanced when BDC2.5 effectors were transferred into Treg-cell-deficient *Cd28*$^{-/-}$ mice (Tang et al., 2006), consistent with previously published results issuing from related experimental manipulations (Bour-Jordan et al., 2004). In other cases, although Treg cells did not inhibit the expansion of islet-reactive Teff cells within the PLNs, they did impede their early differentiation at that site, reducing the production of IFN-γ and expression of chemokine receptors (such as CXCR3) needed for migration to the islets (Sarween et al., 2004) or diminishing the fraction of T cells producing tumor necrosis factor (TNF)-α or interleukin (IL)-17 (Tritt et al., 2008). Effects on the survival of differentiated Teff cells within the PLNs have also been postulated (Tritt et al., 2008).

On the other hand, such influences of Treg cells on the priming phase of islet-reactive T cells were not evident in several other

studies on diabetes models, as LN Teff cells were found to proliferate equivalently in their presence or absence (e.g., Chen et al., 2005). Despite some initial technical difficulties in finding them, it is now clear that Treg cells are prominent residents of many types of autoimmune tissular infiltrates, both murine and human (Zheng and Rudensky, 2007; Sakaguchi et al., 2008). Some investigators have argued that they are inoperative in such an inflammatory context, given that tissue damage eventually occurs (e.g., Korn et al., 2007), but this conclusion ignores the fact that destruction might have been worse in their absence. Treg cells are readily found in prediabetic islet infiltrates, where they have a distinct phenotype, prompting us to propose that such tissue-resident regulatory cells are a key element in local immunoregulation, capable of staving off the terminal destruction of islet β cells for a protracted period (Chen et al., 2005; Herman et al., 2004).

Some of the discrepancies highlighted above no doubt issue from the experimental strategies chosen in the different studies. Transfer systems, employed in most of the experiments, may not mimic the natural disease course, especially when they entail lymphopenic mice as T cell recipients. Chen et al. (2005) tried to sidestep this issue by introducing the *scurfy* (Foxp3-deficiency) mutation into the BDC2.5 TCR transgenic diabetes model, but it is possible that immune system adaptation takes place in the constitutive absence of Treg cells. We have now addressed this issue using a more definitive approach: BAC transgenic mice expressing the diphtheria toxin (DT) receptor (R) under the dictates of *Foxp3* transcriptional regulatory elements were generated directly on the NOD genetic background, allowing temporally controlled ablation specifically of Treg cells. Exploiting this new resource, we have assessed where and how Treg cells impact on the anti-islet autoimmune response. The strength and synchrony of the rapidly ensuing reaction were instrumental in elucidating the pathway by which Treg cells keep the immune system at bay. In particular, it became feasible to study how Treg cells dampen effector cells within the insulitic lesion to stave off the conversion of insulitis to diabetes, a therapeutically critical disease juncture. Unexpectedly, an effect of Treg cells on innate immune system players, notably NK cells, appears to be an early and crucial event.

RESULTS

An Ongoing Need for Treg Cells to Guard against Autoimmune Destruction of the Pancreatic Islets

Controlled lineage ablation is a powerful approach for determining the role of particular cell types in specialized biological processes. More and more, transgene-directed expression of the human DTR in particular cells in mice is being exploited to achieve this goal: murine cells are resistant to DT for lack of a receptor, so those expressing the DTR transgene are uniquely sensitive to DT treatment in vivo (Saito et al., 2001). Importantly, since the death induced by this drug is apoptotic, cell ablation has not provoked an inflammatory response in the many contexts so far examined (Bennett and Clausen, 2007; Feuerer et al., 2009). Recently, this strategy was successfully employed to selectively eliminate Treg cells in mice (Kim et al., 2007; Lahl et al., 2007; Lund et al., 2008).

We generated a Foxp3-DTR line directly on the NOD genetic background by injecting NOD embryos with a large BAC construct harboring a chimeric DTR-eGFP-stop coding segment inserted between the first and second codons of the *Foxp3* open reading frame (Figure S1A available online). Multiple founders expressing GFP in $CD4^+CD25^+$ T cells were obtained, one of which was used to propagate a stable line (NOD.Foxp3^{DTR+}). Two consecutive daily administrations of DT into young adults of this line resulted in an 80%–90% depletion of the $Foxp3^+$ T cells in lymphoid organs such as the spleen, axillary LN, and PLN (data not shown, but see below). By 3 days after the last injection, Treg cell numbers had recovered to a substantial degree (to only ~60% depletion) (data not shown). On one hand, if DT was administered to young adults every other day until day 9 and histological analysis was performed on day 12, only very mild infiltrates were detected in the lung and liver of Foxp3-DTR transgenic mice (but not of transgene-negative littermate control animals) (Figure S1B). On the other hand, the pancreatic islets of the DT-injected transgenic mice showed a strong immune infiltrate at that time-point after treatment, in contrast to the identically treated littermate controls.

The goal of this study was to elucidate the role of Treg cells in controlling the progression of autoimmune diabetes. To that end, we crossed the Foxp3-DTR transgene into the BDC2.5 TCR transgenic mouse model. The BDC2.5 line derives from a $CD4^+$ T cell clone that is restricted by the NOD MHC-class-II A^{g7} molecule and is specific for an unknown pancreatic islet β-cell protein (Katz et al., 1993; Haskins et al., 1988). This line has been instrumental in elucidating the constellation of immunoregulatory genes, molecules, and cells that control the frequency and aggressivity of diabetogenic T cells (Gonzalez et al., 1997; Luhder et al., 1998; Kanagawa et al., 2002; Poirot et al., 2004). In BDC2.5 mice, T cells invade the islets at 15–18 days of age and seed a massive infiltration therein; however, on the NOD genetic background, progression to diabetes occurs only months later in only 10%–20% of animals, reflecting strong immunoregulation at play. Thus, this model has the attractions of being well studied, having a T cell compartment that can be easily tracked, being conveniently synchronous, and exhibiting readily discernable immunoregulation.

BDC2.5/NOD.Foxp3^{DTR+} double-transgenic mice showed an efficiency of Treg cell depletion, including ablation of the population residing in the pancreas, similar to that mentioned above for the polyclonal NOD.Foxp3^{DTR+} animals (Figure 1A). In a first set of experiments, the double-transgenic mice were assessed 24, 72, and 120 hr after the depletion of Treg cells. As documented in Figure 1B, histological changes could be observed as early as the 24 hr time point. The innocuous, static-looking infiltrate characteristic of negative-control mice had begun to evolve such that the leukocyte mass seemed to breach its boundaries and infiltrate deeply into the islet space. In addition, the border between the endocrine and exocrine tissue became much more fuzzy (second row of panels, arrowhead). After 72 hr, the leukocytes appeared to aggressively swarm throughout the islets, even beginning to invade the exocrine pancreas (third row, arrowhead). During the next 2 days, the islet completely disaggregated, making it difficult to recognize β cells, and the infiltrate escaped massively into the exocrine tissue (bottom row, arrowhead). This picture is very reminiscent of what we previously

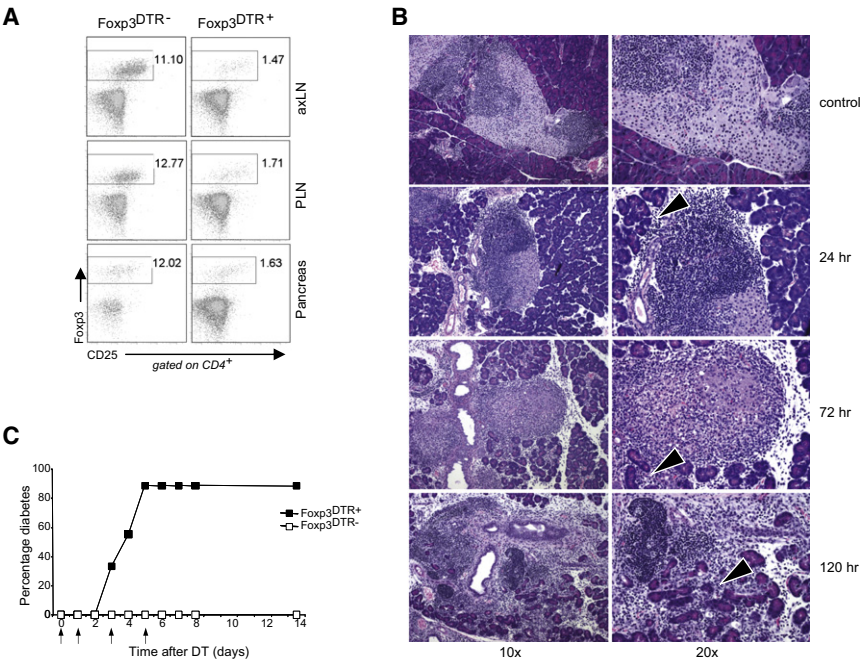

Figure 1. Kinetics of the Autoimmune Attack on the Pancreas

(A) NOD.Foxp3^{DTR+} mice were crossed with BDC2.5 TCR tg mice (Katz et al., 1993), and Treg cell depletion was analyzed. Percentage of Treg cells after two daily injections of DT into BDC2.5/NOD.Foxp3^{DTR+} and DTR^{-} control littermates is shown. Representative dot plots for axillary LN (axLN), PLN, and pancreas tissue are shown.

(B and C) DT injections into 4- to 5-week-old BDC2.5/NOD.Foxp3^{DTR+} mice induced a rapid onset of diabetes. (B) Histological sections of pancreas tissue after H&E staining, with two different magnifications of the same area: 10× objective left column and 20× objective right column. (B, upper panel) BDC2.5/NOD.Foxp3^{DTR-} control animal 120 hr after DT treatment. (B, middle and lower panels) BDC2.5/NOD.Foxp3^{DTR+} mice analyzed at different time points after DT treatment: 24 hr, 72 hr, and 120 hr. Arrowheads indicate text-cited areas of infiltration. Representative sections are shown. (C) Diabetes incidence of BDC2.5/NOD.Foxp3^{DTR+} (n = 9) and DTR-negative control littermates (n = 9) after DT treatment as described in Experimental Procedures. Arrows indicate days of DT injection.

documented for Foxp3-defective and Rag-deficient BDC2.5 TCR transgenic mice (Chen et al., 2005).

In agreement with these findings, diabetes occurred as soon as 3–5 days after the punctual ablation of Treg cells from adult BDC2.5/NOD.Foxp3^{DTR+} mice (Figure 1C), clearly demonstrating an ongoing need for Treg cells to guard against autoimmune attack of the pancreas.

The Removal of Treg Cells Activates Teff Cells Predominately within the Pancreas

Given the strength and synchrony of the disease that rapidly developed subsequent to Treg cell depletion, this system seemed a highly advantageous one for elucidating how Treg cells rein in Teff cells in the T1D context. First, we asked where Treg cells were having the greatest effects: in the PLNs, the site of ongoing T cell priming, or within the insulitic lesion itself? We initially employed microarray gene-expression profiling as a broad, unbiased approach to addressing this question, focusing on CD4^{+} T cells because they are the primary effector cells in the BDC2.5 model. Non-Treg T cells were sorted as GFP-negative at 0, 15, and 24 hr after a single injection of BDC2.5/NOD.Foxp3^{DTR+} mice and BDC2.5/NOD.Foxp3^{DTR-} littermate controls with DT. RNA samples were prepared in triplicate and were hybridized to Affymetrix M430v2 microarrays, and RNA-normalized expression values were analyzed. (Datasets have been deposited at NCBI-GEO under accession no. GSE18136.)

A global comparison of gene-expression values revealed that far more extensive changes occurred in the pancreas-derived CD4^{+} Teff cells than in their PLN counterparts: at an arbitrary counting threshold of 2-fold changes, 352 genes were overexpressed in the pancreas 24 hr after Treg cell ablation, while 168 genes were underrepresented, versus 46 and 26, respectively, in the PLN (Figure 2A, left panels; Table S1). A direct comparison of transcript alterations in a fold change-fold change (FC-FC) plot demonstrated that many of the same changes occurred in the pancreas and the PLNs, but the off-diagonal alignment (slope = 0.36) confirmed the dominant pancreas response (Figure 2B, left panel). At 15 hr, CD4^{+} Teff cells from both sites exhibited only minor alterations in gene expression (Figures 2A and 2B, right panels); however, highlighting on the 15 hr plots those genes whose expression had changed by 24 hr revealed that the response was already beginning at the earlier time point for certain loci, with a bias for both overexpressed (in red) and underrepresented (in blue) genes (Figure 2C). Thus, elimination of Treg cells had a dominant impact within the insulitic lesion, rather than in the draining lymph nodes, and the response was surprisingly rapid, discernible by as few as 10–12 hr or so (considering that the death of Treg cells in response to DT must take at least a few hours).

To begin characterizing the effects on Teff cells, we highlighted on the FC-FC plot of Figure 2D a T cell activation-proliferation signature previously defined on the basis of compiled analyses of T cells stimulated by antigen in vitro or in vivo (Hill et al., 2007). At 24 hr after Treg cell depletion, transcripts of the activation-proliferation signature were clearly altered in the pancreas, but far less so in the PLN. There was little to no change in this signature at 15 hr. For an independent verification of these conclusions, we isolated CD4^{+} T cells from the pancreas and PLN at 15, 20, and 24 hr after Treg cell removal and analyzed them by flow cytometry for expression of the early activation marker CD69 (Figure 2E). Pancreas-resident CD4^{+} T cells showed an increase in cell-surface display of CD69 between 15 and 20 hr, consistent with the gene-expression profile. As expected, PLN-derived CD4^{+} T cells did not exhibit a significant change in CD69 expression at these early time points.

Because the highlighted signature included proliferation-associated transcripts, we confirmed the above conclusions in

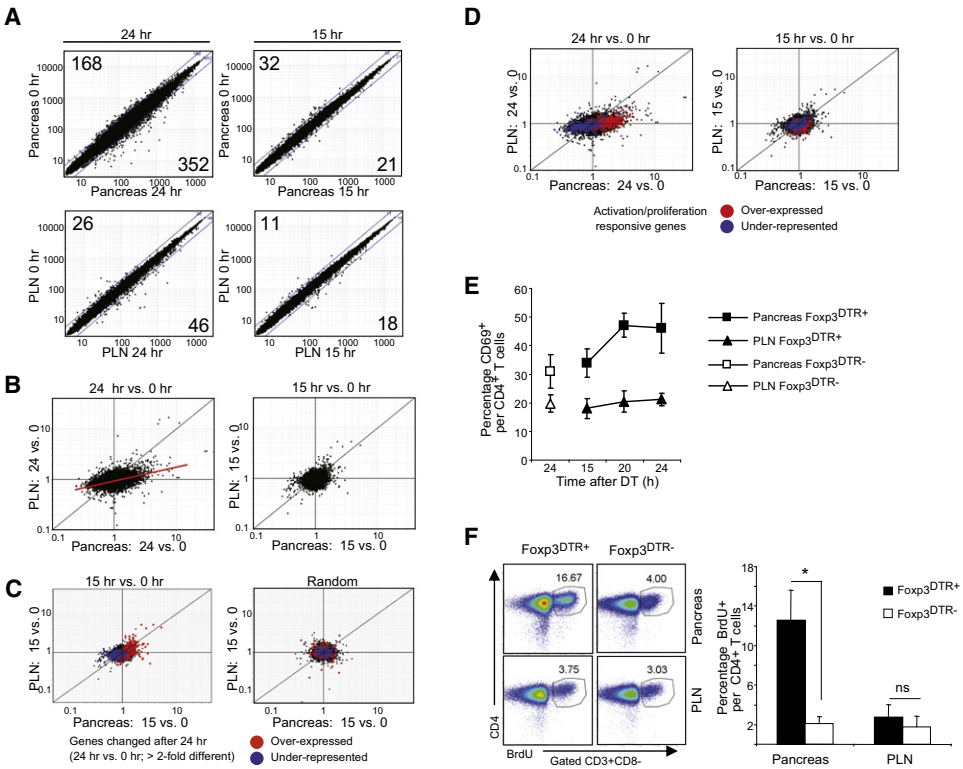

Figure 2. T Cell Activation and Proliferation in the Pancreatic Lesion

(A–D) Affymetrix M430 2.0 microarray data. $CD4^+$ T cells were isolated from the pancreas lesion and PLN at three different time points: 0, 15, and 24 hr after DT treatment from BDC2.5/NOD.$Foxp3^{DTR+}$ mice. (A) Expression versus expression values are plotted for pancreas and PLN at 24 and 15 hr. Numbers indicate count of probes that were differentially expressed more than 2-fold. (B–D) Fold change to fold-change plot. (B) 24 hr versus 0 hr for PLN and pancreas (left panel) and 15 hr versus 0 hr for PLN and pancreas (right panel). Red line (in left panel) represents the linear regression curve. (C) Gene changes after 24 hr (and presented in Table S1) are highlighted in the 15 hr versus 0 hr PLN versus pancreas plot (left panel) and random data control (right panel). (D) Activation and proliferation responsive genes (Hill et al., 2007) overexpressed (red) or underrepresented (blue) are highlighted in 24 hr versus 0 hr for PLN and pancreas (left panel) and 15 hr versus 0 hr for PLN and pancreas (right panel).

(E) $CD4^+$ T cells were stained for the early activation marker CD69 at different time points after DT treatment from pancreas and PLN, from BDC2.5/NOD.$Foxp3^{DTR+}$ (filled symbols) and BDC2.5/NOD.$Foxp3^{DTR-}$ control mice (open symbols).

(F) BrdU staining of $CD4^+$ T eff cells: BrdU was injected 48 hr after DT treatment and mice were analyzed after 1 hour. Pancreas and PLN from BDC2.5/NOD.$Foxp3^{DTR+}$ or DTR-negative control mice were stained for BrdU and CD4. Left panel shows representative dot plots, right panel summarizes four to five mice from independent experiments with mean and SD. *Significant difference ($p < 0.05$).

bromodeoxyuridine (BrdU)-labeling experiments. Mice were intravenously (i.v.) injected with BrdU 48 hr after DT administration, the pancreas and PLN were excised 1 hour later, and cells were stained for incorporation of BrdU into their DNA as an indicator of proliferation. We chose this very early time point to exclude the possibility of division elsewhere followed by labeled cell migration into the pancreas. Again, pancreas-resident $CD4^+$ T cells showed a substantial early reaction: about 13% were in S phase during the labeling period, compared with only about 2% in the DT-treated DTR-negative littermate control group (Figure 2F). In contrast, the division of PLN-derived $CD4^+$ T cells was not significantly different from that of their negative control counterparts. The dichotomy in proliferation was also seen with $CD8^+$ T cells from the pancreas versus PLN, with high rates in the former and less increase in the latter (Figure S2).

By these diverse criteria, then, Treg cell ablation can unleash a rapid activation of $CD4^+$ Teff cells residing within the autoimmune lesion while not in the draining LNs.

The $CD4^+$ Teff Cell Response Unleashed by Treg Cell Depletion

Thus, Treg cells restrain Teff cells within the insulitic lesion, inhibiting terminal destruction of the mass of β cells. But what are the critical effector functions thereby kept in check? And what molecules drive these functions? Many of the genes highly induced in response to Treg cell ablation are implicated in the function of known Th subsets, notably transcripts encoding Tbet (3.8-fold overexpressed), IL-12rb1 (2.3-fold), IFN-γ (9.9-fold), granzyme B (6.1-fold), and granzyme A (2.6-fold) for Th1 cells and IL-17 (2.3-fold), IL-22 (9.3-fold), and IL-21 (3.7-fold) for Th17 cells (Figure 3A and Table S1). A number of these alterations were confirmed by flow-cytometric or quantitative-PCR analysis. For example, monoclonal antibody (mAb) staining for intracellular IFN-γ and IL-17 showed an increase in pancreas Teff cells at 48 hr after Treg cell depletion, and also an augmentation in IFN-γ production in PLN cells at this later time point (Figures 3B and 3C). In contrast, there were no evident differences in

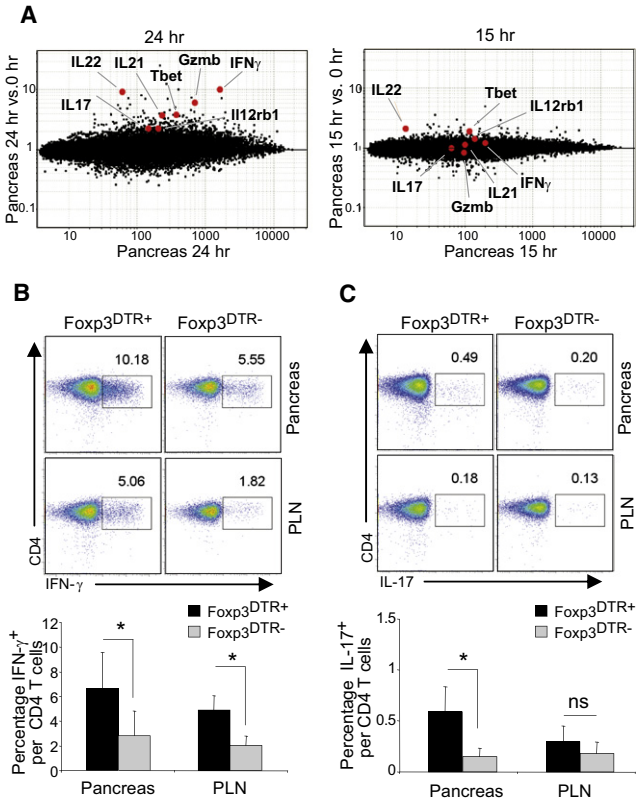

Figure 3. Molecular Changes after Treg Cell Ablation

(A) Microarray data showing fold change versus expression value plot for 24 hr versus 0 hr (left panel) and 15 hr versus 0 hr (right panel) for T cells isolated from the pancreas. Some overexpressed genes are highlighted.

(B and C) Cytokine expression of $CD4^+$ T cells from pancreas and PLN, 48 hr after DT injection into BDC2.5/NOD.$Foxp3^{DTR+}$ or DTR-negative control mice. (B), IFN-γ; (C), IL-17. Upper panel, dot plots; lower panel, summary of four mice per group with mean + SD. *Significant difference ($p < 0.05$).

the intracellular expression of TNF-α, IL-4, IL-10, and IL-2 in pancreas Teff cells (Figure S3).

We wondered whether IFN-γ might be an important "driver" cytokine because (1) transcripts encoding Tbet, which induces this cytokine's expression, were upregulated in pancreas $CD4^+$ Teff cells already at 15 hr after Treg cell ablation (Table S1); (2) transcripts encoding IFN-γ, itself, though not yet induced in this population at 15 hr, were strongly upregulated by 24 hr (Table S1), and more of the cells were actually producing this cytokine (Figure 3B); and (3) isolated BDC.2.5 Th1 cells rapidly provoke autoimmune diabetes upon transfer (Katz et al., 1995). Thus, we overlaid an IFN-γ-response signature (independently derived [J. Wu, D.M., C.B., unpublished data]) onto the p value versus FC "volcano" plots of the $CD4^+$ T cell expression values. A clear displacement of the IFN-γ-induced (red) and IFN-γ-repressed (blue) transcripts was already evident at 15 hr (Figures 4Ai and 4Aii; $p = 4.85^{-16}$). A control TGF-β signature showed no such bias—if anything, the TGF-β-induced transcripts were slightly underrepresented (Figures 4Aiii and 4Aiv).

Subsequent to Treg cell ablation, IFN-γ-responsive genes were upregulated in $CD4^+$ Teff cells faster than the genes of the activation signature were and faster than the *Ifng* gene itself was (Figure 4B, upper and lower panels), prompting us to search for other cells producing this cytokine. We performed a careful kinetic analysis around this early time point, quantifying IFN-γ transcript levels in $CD4^+$, $CD8^+$, and NK cells from various organs (Figure 4C). All cell types from all organs of the DT-treated DTR-negative littermate controls showed background levels of IFN-γ transcripts at all of the time points. Unexpectedly, NK cells exhibited the earliest, greatest response. There was a burst of *Ifng* expression by NK cells from the insulitic lesion as soon as 15 hr after DT injection, which was barely detectable in the PLN NK cells and was undetectable in the spleen NK population. In clear contrast, IFN-γ transcripts were not upregulated in either $CD4^+$ or $CD8^+$ cells at this time point, but only after a lag of about 9 hr, though only in the lesion and never reaching the expression in NK cells.

NK Cells Sense the Loss of Treg Cell Control

The striking induction of IFN-γ expression by NK cells in response to declining Treg cell numbers suggested that this innate immune system cell type might play a primordial role in diabetogenesis in this setting. We first addressed this possibility by analyzing the percentage, proliferation, and effector molecule expression of NK cells in the PLN and pancreas during the course of Treg cell ablation. The percentage of NK cells in the pancreas steadily increased along with the decrease in Treg cells, rising from about 2% to about 10% by 48 hr, with the first significant augmentation ($p = 0.048$) occurring between 15 and 20 hr after the initial administration of DT (Figure 5A, upper and lower panels). The rise in NK cells in the PLN was more moderate and lagged somewhat behind, a substantial increase not being apparent until 48 hr (Figure 5A, lower panel). BrdU-labeling experiments at 48 hr revealed NK cells in both the pancreas and PLN to be actively proliferating (Figure 5B). Again, the short (1 hr) BrdU pulse argued that the bulk of the BrdU labeling represented in situ proliferation rather than an influx of cells that had divided elsewhere.

We wondered whether the induction of IFN-γ synthesis by NK cells was accompanied by an increase in the NK-cell killing potential as well. Indeed, PCR analysis at 24 hr after DT-injection did show an augmentation in transcripts encoding granzymes A and B, especially in the insulitic lesion, and less so in the PLN (Figure 5C). While *Gzma* mRNA was expressed essentially only in NK cells, *Gzmb* transcripts were upregulated in pancreatic $CD4^+$ and $CD8^+$ T cells in addition (data not shown). An in vivo cytoxicity assay confirmed the unleashing of NK cell activity upon Treg cell ablation (Figure 5D). DTR-positive or DTR-negative BDC2.5/NOD mice were depleted of Treg cells two days before injection of a mix of splenocyte populations ($CFSE^{lo}$ MHCI-negative targets and $CFSE^{hi}$ MHCI-positive controls); sixteen hours later, NK cell activity in different organs was measured by comparing the ratio of the two populations. NK activity was significantly enhanced after Treg cell depletion, in the pancreatic tissue ($p = 0.017$) and draining LN ($p = 0.0058$), and also in the spleen at this rather late time point. These results provide important evidence that Treg cell ablation impacts on NK cell activity itself and in an in vivo context.

The IFN-γ Induction Triggered by a Loss of Treg Cells Is Prodiabetogenic

We have shown, then, that specific, punctual depletion of Treg cells provoked a rapid rise in NK cell production of IFN-γ in

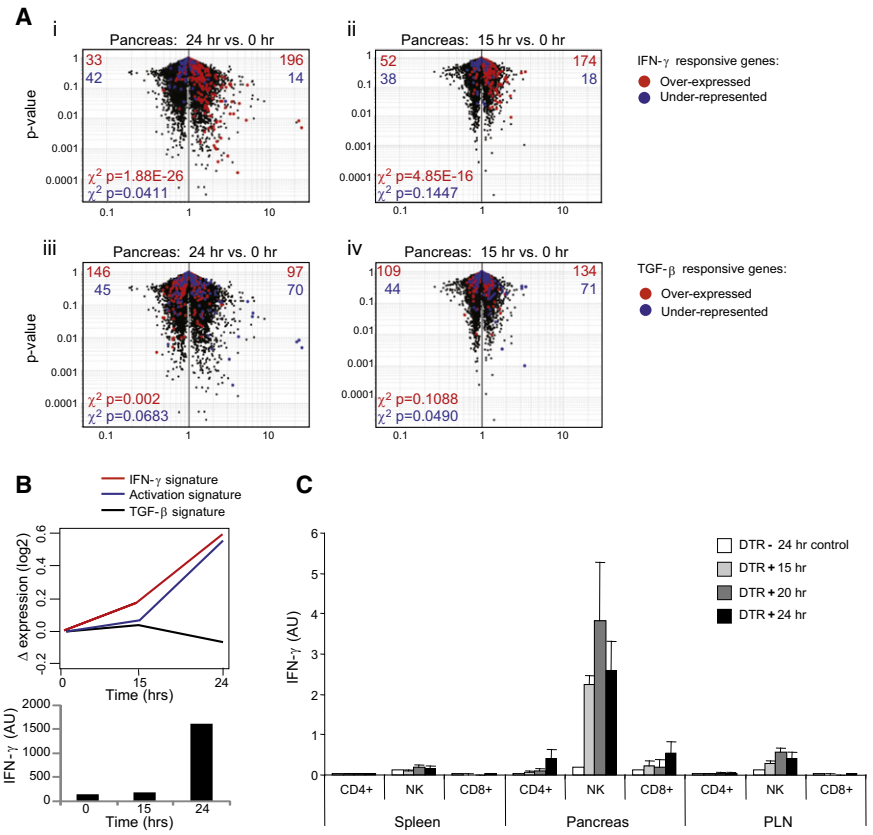

Figure 4. Induction of IFN-γ Expression Is An Early, Predominant Response after Punctual Treg Cell Depletion

(A) $CD4^+$ T cells were isolated from the pancreas at three different time points: 0, 15, and 24 hr after DT treatment from BDC2.5/NOD.$Foxp3^{DTR+}$ mice. (Ai–Aiv) p value versus fold change (FC) "volcano" plot for the pancreas $CD4^+$ Teff population at 24 and 15 hr after DT treatment. IFN-γ-responsive genes (Bi and Bii) or TGF-β-responsive transcripts (Aiii and Aiv) either upregulated (red) or downregulated (blue) by the respective cytokine were highlighted. p values presented within the graphs (Ai–Aiv) were calculated (χ^2 analysis) based on the number of genes dropping to the left or right side of the FC distribution (colors indicate upregulated [red] or downregulated [blue] genes). Red or blue digits in the upper corner of each plot indicate the number of probes on each side of the distribution. (Ai) and (Aiii) at 24 hr; (Aii) and (Aiv) at 15 hr.

(B) Upper panel: Log2 delta expression values of (15 hr − 0 hr) and (24 hr − 0 hr) for genes from three different signatures: IFN-γ (red), activation/proliferation (blue), and TGF-β (black). Lower panel: IFN-γ expression in $CD4^+$ Teff cells isolated from the pancreas at 0, 15, and 24 hr after DT.

(C) Quantitative PCR for IFN-γ expression. $CD4^+$, NK, and $CD8^+$ cells were isolated from spleen, pancreas, and PLN from BDC2.5/NOD.$Foxp3^{DTR+}$ or DTR-negative control mice at different time points (15, 20, and 24 hr) after DT injection. Data are expressed as arbitrary units (AU), and the mean + SD from four independent experiments are shown.

pancreas tissue targeted by autoimmunity, which in turn substantially impacts on the gene expression program of the pancreas-resident $CD4^+$ Teff cells. The implication is that IFN-γ is an important trigger of diabetogenesis in this context, a notion we tested by performing mAb blocking studies. Anti-IFN-γ was administered coincident with the DT treatment, and its effects were monitored 24 hr later. One consequence was a substantial reduction in the augmentation of pancreatic NK cells usually provoked by Treg cell ablation (Figure 6A). In addition, there were effects on the expression of effector genes in NK and other cell populations. The induction of *Ifng* gene transcription in NK cells, $CD4^+$ T cells, and $CD8^+$ T cells in the pancreas that usually occurred in the absence of Treg cells was inhibited (Figure 6B). The induction of Th17 effector cytokines was attenuated even more, suggesting that they might be a downstream event (Figure 6C). Importantly, the diabetes normally triggered by Treg cell ablation was strongly inhibited by IFN-γ blockade, being both delayed and less frequent (Figure 6D).

Lastly, we sought to establish a role for NK cells themselves in unleashing Teff cell activities. Treatment with reagents specific for asialo-Gm1 or NKp46 did not lead to effective NK-cell depletion. Therefore, we introduced the NK1.1 marker into the BDC2.5/NOD.$Fox3^{DTR}$ line by crossing it with a NOD.NK1.1 congenic line (Carnaud et al., 2001). As expected, ablation of Treg cells from the F1 mice by DT treatment for 24 hr resulted in an augmented population of NK cells, which was substantially depleted by coadministration of anti-NK1.1 (Figure 7A). There were accompanying reductions in the expression of the genes encoding both IFN-γ and granzyme-B by pancreatic $CD4^+$ T cells (Figure 7B), reductions that correlated nicely with the loss of NK cells (Figure 7C). In contrast, the expression of granzyme B by the remaining NK cells was unaltered (Figure 7B), arguing for its independence of NK-cell-produced mediators (notably IFN-γ).

DISCUSSION

This study addressed where and how Treg cells impact on autoimmunity, in particular the autoimmune attack on the pancreatic islets that preludes T1D. We chose a punctual loss-of-function approach that permitted specific, controlled elimination of Treg cells in prediabetic BDC2.5/NOD mice with an ongoing, but contained, insulitis. Acute Treg cell ablation had a devastating effect in this context: within hours, the "well-behaved" leukocytes within the insulitic lesion were unleashed, culminating in armed effector cells that rapidly executed terminal destruction of the mass of islet β cells. The strength and synchrony of this response facilitated dissection of the intervening molecular and cellular events. The earliest and most striking changes subsequent to Treg cell depletion were observed within the infiltrated islets rather than in the allied lymphoid tissue. An activated, expanding population of NK cells drove an early increase in the production of IFN-γ, which had a dominant impact on the gene-expression

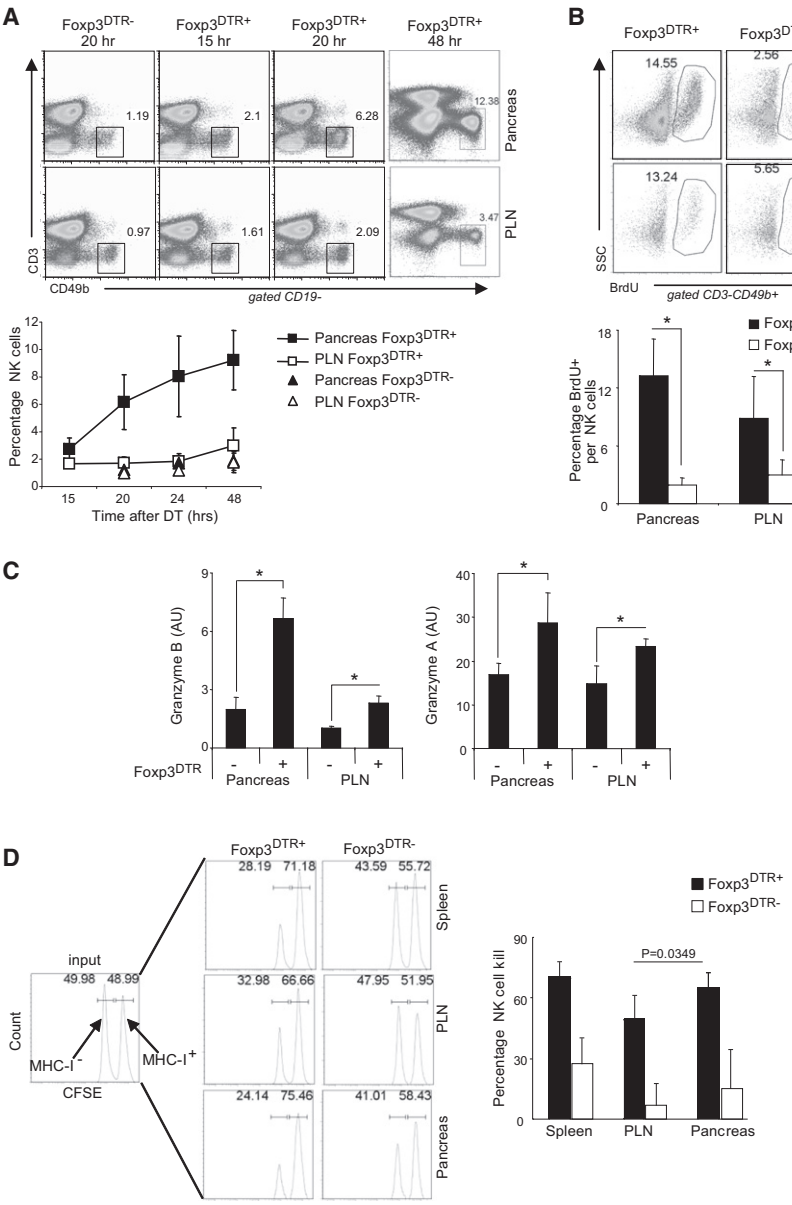

Figure 5. The Loss of Treg Cell Control Triggers NK Cell Activation within the Autoimmune Lesion

(A) Accumulation of NK cells in autoimmune lesions. NK cells were identified as $CD19^{-}CD3^{-}CD49b^{+}$ in the lymphocyte gate. Presence of NK cells was followed in BDC2.5/NOD. $Foxp3^{DTR+}$ or DTR-negative control mice 15, 20, 24, and 48 hr after DT application in pancreas and PLN. Upper panel: representative dot plots are shown. Lower panel: mean and SD of four to six independent experiments per group and time point are presented.

(B) BrdU incorporation (as described in the legend to Figure 2F). Upper panel shows representative dot plots, and lower panel summarizes four to five mice from independent experiments with mean and SD. *Significant difference ($p < 0.05$).

(C) Quantitative PCR data for granzyme B (left panel) and granzyme A (right panel) expression in NK cells, isolated from pancreas and PLN from BDC2.5/NOD.$Foxp3^{DTR+}$ or DTR-negative littermate control mice at 24 hr after DT injection. Data are expressed as arbitrary units (AU). The mean + SD from three to four independent experiments are shown. *Significant difference ($p < 0.05$).

(D) In vivo NK cell cytotoxicity assay. DTR-positive or DTR-negative BDC2.5/NOD mice were depleted of Treg cells 2 days before injection of a mix of splenocyte populations ($CFSE^{lo}$ MHCI-negative targets and $CFSE^{hi}$ MHCI-positive controls); 16 hr later, NK cell activity was measured by comparing the ratio of the two populations in spleen, PLN, and pancreas. Left panel, representative dot plots. Right panel summarizes three independent experiments with mean and SD. NK cell cytotoxicity was significantly different in all organs (DTR^{+} versus DTR^{-}). Significant difference ($p = 0.0349$) between PLN and pancreas in the DTR-positive group.

program of $CD4^{+}$ T effector cells and ultimately provoked the development of clinical diabetes.

It may be instructive, first of all, to consider these findings in the context of previously reported experiments entailing punctual ablation of Treg cells. Inserting a DTR-encoding construct into the endogenous Foxp3 locus, which resulted in ~98% depletion of this regulatory population, the Rudensky group found Treg cells to be required throughout life to avoid autoimmunity in C57Bl/6 (B6) (non-autoimmunity-prone) mice: in their absence, a devastating multiorgan autoimmune disease developed in 1 to 2 weeks (Kim et al., 2007; Lund et al., 2008). Quite different results were published by Lahl et al. (2007), who employed a DTR-BAC strategy that resulted in only about 90% Treg cell depletion: although B6 neonates lacking this population developed raging autoimmunity, adults did not. Apparently, even a small Treg cell compartment is capable of controlling this form of autoimmunity in adult mice. Our experimental system proved to be rather like that of Lahl et al. DT treatment of the NOD.$Foxp3^{DTR+}$ line resulted in 80%–90% elimination of Treg cells; in 4-week-old NOD individuals, not yet showing signs of the insulitis that ultimately afflicts 100% of NOD mice, Treg cell depletion to this degree led to mild leukocytic infiltrates in the lung and liver, accompanied by strong invasion of the pancreas, but only after 12 days. Thus, the interpretation of results from our system should not be confounded by the side-effects of devastating systemic autoimmunity. Another point to keep in mind is that autoimmunity is already installed in our system, based on prediabetic BDC2.5/NOD mice, so that a lymph node priming event triggered by the loss of Treg cells is not a requirement for disease to initiate. This is most likely the reason why we saw autoimmune manifestations already within hours, rather than in the several days reported for the B6 systems (Kim et al., 2007; Lund et al., 2008).

A key, somewhat unexpected finding was the early activation of NK cells after Treg cell depletion, resulting in their expansion,

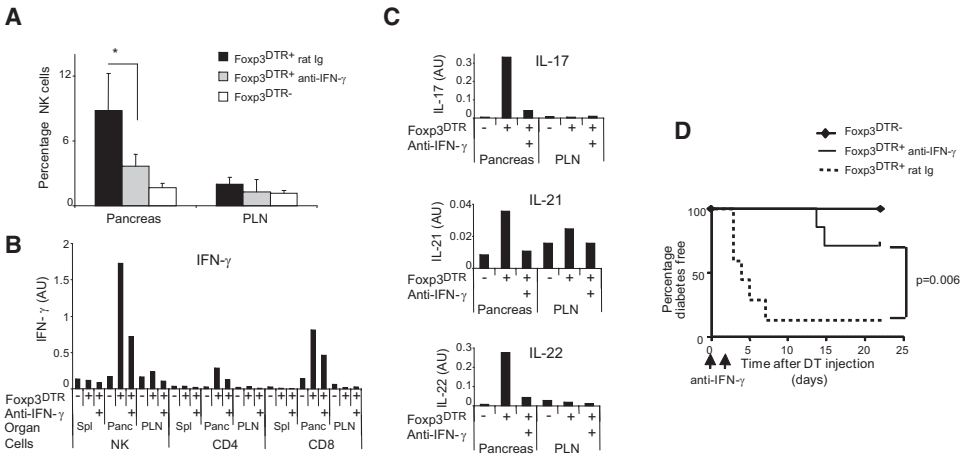

Figure 6. IFN-γ Drives the Autoimmune Response Provoked by Treg Cell Removal

(A–C) BDC2.5/NOD.Foxp3^{DTR+} or DTR-negative control mice were treated with DT and injected with anti-IFN-γ or control rat Ig (0.5 mg). Cells were isolated 24 hr after treatment from pancreas and PLN. (A) Decreased NK cell accumulation in anti-IFN-γ-treated group. Summary of four mice per group and organ with mean and SD is shown. *Significant difference ($p < 0.05$). (B) Quantitative PCR data from NK, CD4$^+$ and CD8$^+$ cell for IFN-γ expression. Data are expressed as arbitrary units (AU); one representative experiment out of two is shown. (C) Quantitative PCR data for IL-17, IL-21, and IL-22 from CD4$^+$ T cells isolated from pancreas and PLN. Data are expressed as arbitrary units (AU), and one representative experiment out of two is shown.

(D) Diabetes incidence of BDC2.5/NOD.Foxp3^{DTR+} and DTR$^-$ control animals after DT treatment as described in Experimental Procedures. Foxp3^{DTR+} group was split into anti-IFN-γ or control rat Ig (1 mg) treated set. Seven to eight mice per group and treatment are displayed. p value was calculated with log-rank test for survival curves. Arrows indicate days of antibody injection.

a burst of IFN-γ production as rapidly as 15 hr later, and subsequent expression of effector molecules such as granzymes A and B. Teff cells responded very rapidly to the increase in IFN-γ, and their ultimate destructiveness toward islet β-cells depended on it. It is not yet known to what extent β-cell death might also depend on the direct killing function of NK cells, perhaps via granzyme activity. While NK cells have recently been reported to control the destructiveness of insulitis in a few particularly aggressive models of autoimmune diabetes (Poirot et al., 2004; Alba et al., 2008), there has been little hint that their behavior is kept in check so immediately and powerfully by Treg cells. That NK cells can be subjugated by Treg cell control has been reported in other contexts. They become activated and/or expand in mice constitutively or punctually depleted of Treg cells (Kim et al., 2007; Terme et al., 2008; Ghiringhelli et al., 2005; Lund et al., 2008), and Treg cells can augment various of their in vivo activities, for example, their proliferation, cytotoxicity, NKG2D receptor expression, and ability to control tumor growth. However, in all of these previous studies, the secondary lymphoid organs were the focus of attention, and NK cells were thought to join the action rather late, subsequent to, and dependent on critical interactions between DCs and CD4$^+$ Teff cells (Kim et al., 2007; Terme et al., 2008). The early involvement of NK cells in the diabetogenic process provoked by Treg cell depletion in the BDC2.5/NOD system most likely reflects their prerecruitment to the insulitic lesion and at least partial activation therein. It is not yet clear whether the Treg cells act directly on NK cells to dampen IFN-γ production, as they have been seen to do in vitro in a different disease setting (Ghiringhelli et al., 2005). Alternatively, they might operate through the intermediary of DCs, perhaps keeping in check an IL-12-IFN-γ feed-forward loop, reminiscent of what is being observed in more and more experimental settings (Martin-Fontecha et al., 2004; Wu et al., 2007). Indeed, our most recent studies on even earlier time points after Treg cell ablation (illustrated in Figure S4) revealed induction of the *Ifng* gene in pancreatic NK cells already at 7 hr after DT treatment, followed shortly thereafter (12 hr) by an increase in DC expression of the *Il12b* gene. Anti-IL-12p40 treatment reduced, though did not extinguish, *Ifng* gene expression by NK cells, but did not influence granzyme B expression over the same time-frame.

Thus, Treg cell control of IFN-γ production, and thereby effector cell activities directly within infiltrated islets of BDC2.5/NOD mice, seems to be an important element of their prolonged restraint of the progression of insulitis to overt diabetes. This conclusion does not mean, however, that in the setting of unmanipulated mice, BDC2.5, or other, the long-delayed spontaneous emergence of effector cells from Treg cell control and development of diabetes necessarily requires IFN-γ. Indeed, NOD mice show only mild disease attenuation in the absence of IFN-γ or IFNγ-R (Hultgren et al., 1996; Kanagawa et al., 2000; Serreze et al., 2000), although, on the other hand, injection of an anti-IFN-γ was found to have a strong effect (Debray-Sachs et al., 1991), T-bet is a requirement (Esensten et al., 2009), and IFN-γ-producing Th1 cells potently induce disease on transfer (Katz et al., 1995). It may be that Treg cell control of IFN-γ production keeps the autoimmune lesion in check for a protracted period (and in its absence diabetes is immediate and intense), but that with time, effector cells bypass this restraint and proceed to decimate the β cells by an IFN-γ-independent mechanism. An obvious possibility would be through the slow emergence of a Th17 or similarly autoaggressive population. The emergent population might be less effectively controlled by Treg cells, so such a switch could explain observations of a reduced susceptibility of CD4$^+$ Teff cells to Treg cell suppression in aging NOD mice as they develop clinical diabetes (You

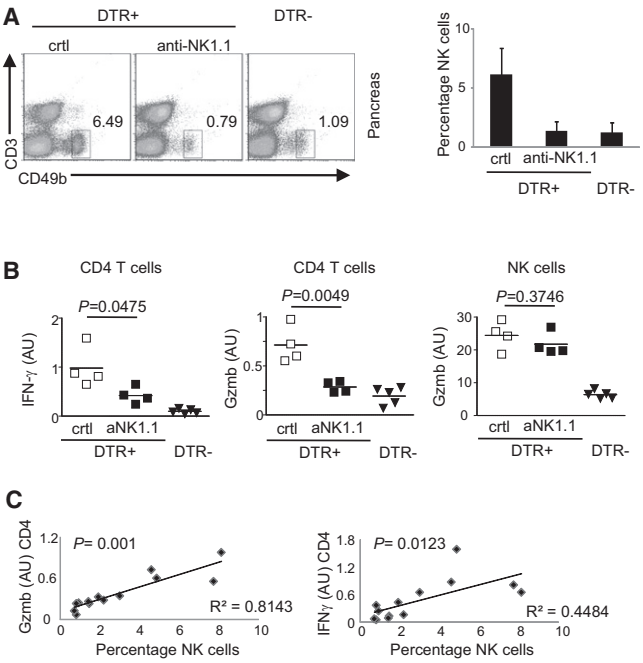

Figure 7. NK Cells Directly Influence CD4$^+$ T Cell Activation after Treg Cell Removal

BDC2.5/NOD.Foxp3^{DTR} line was crossed with NK1.1-congenic NOD mice, and anti-NK1.1 (0.5 mg) was injected to efficiently deplete NK cells in NK1.1$^+$ offspring. Data shown are derived from the pancreas.

(A) Accumulation of NK cells in the autoimmune lesion and NK cell depletion efficiency. The presence of NK cells was followed in BDC2.5/NOD.Foxp3^{DTR+} or DTR-negative control mice 24 hr after DT application in pancreas; anti-NK1.1 represents the anti-NK1.1-treated group, and crtl represents control group. Left panel: representative dot plots are shown. Right panel: mean + SD of four to five mice per group are presented.

(B) Quantitative PCR data from CD4$^+$ and NK cells for IFN-γ and granzyme B (Gzmb) expression isolated from the pancreas and described in (A). Each dot represents an individual mouse.

(C) Quantitative PCR data from CD4$^+$ cell for IFN-γ and granzyme B (Gzmb) expression are plotted against the percentage of NK cells in the pancreas. p values and R^2 were calculated. Each dot represents an individual mouse.

et al., 2005; Gregori et al., 2003). Moreover, it is possible that any such alternative CD4$^+$ Teff cell population might expand in the long-term, but not acute, absence of IFN-γ, thus explaining the discrepancies mentioned above.

Treg-cell-based therapy is currently seen as an attractive strategy for preventing or halting the progression of T1D, as well as multiple other autoimmune disorders. For such an approach to be optimally successful, it will be highly advantageous to know precisely where and how Treg cells are exerting their impact, which may well vary in different disease settings.

EXPERIMENTAL PROCEDURES

Mice

Mice expressing the human DTR under the control of *foxp3* transcriptional control elements (Foxp3^{DTR}) were generated by BAC transgenesis. The BAC construct spanned from 150 kb upstream to 70 kb downstream of the Foxp3 transcription start-site. A DTR-eGFP cDNA with a stop codon was inserted between the first and second codons of the Foxp3 open reading frame. The recombinant Foxp3-DTR-eGFP BAC was injected into NOD fertilized oocytes, and offspring were genotyped by PCR.

NOD-LtDOI (NOD), NOD.Foxp3^{DTR}, and BDC2.5/NOD TCR transgenic mice (Katz et al., 1993) were bred in the specific-pathogen-free facility of the Joslin Diabetes Center. Four-week-old NOD and 4- to 6-week-old female BDC2.5/NOD.Foxp3^{DTR+} mice and BAC-negative control animals were i.p. injected with DT (Sigma, St. Louis, MO) (40 ng/g body weight) and were analyzed at the indicated time points.

For NK cell depletion, the BDC2.5/NOD.Foxp3^{DTR} line was crossed with the NK1.1-congenic NOD line (Carnaud et al., 2001). NK cell depletion was performed by i.p. injection of the depleting mAb against NK1.1 (clone, PK136; 0.5 mg) 1 day before the injection of DT. B2m-deficient NOD mice were used as splenocyte donors in the in vivo NK cytotoxicity assay. IFN-γ was blocked by i.p. injecting anti-IFN-γ mAb (clone, R4-6A2) control rat Ig together with the first injection of DT. Mice received a second injection of anti-IFN-γ mAb on day 2. IL-12p40 was blocked by i.p. injection of mAb against IL-12p40 (clone, C17.8; 0.5 mg) together with the injection of DT. Animal experiments were conducted under protocols approved by the Institutional Animal Care and Use Committees of the Joslin Diabetes Center and Harvard Medical School.

Disease Assays

For histology, the pancreas was excised at different time points after DT injection and was fixed in formalin, and stepped five-micron sections were stained with H&E. For diabetes incidence studies, mice were DT injected on days 0, 1, 3, and 5 (or until diabetes developed, but not longer than 5 days), and diabetes was assessed by measuring blood-glucose levels (350 mg/dl on two consecutive draws).

Cell Sorting and Flow Cytometry

Different leukocyte subsets were isolated from the spleen, PLN, and pancreas at the indicated time points after Treg cell depletion, and the cells were stained with the stated mAbs. In some experiments, leukocytes were sorted directly into Trizol using the Moflo instrument. Isolated RNA was used for quantitative PCR or microarrays.

Cell-surface and intracellular stainings were performed with mAbs against CD3 (clone 145-2C11, BD), CD4 (clone RM4-5, BioLegend), CD8 (clone 5H10; BD), CD19 (clone 6D5; Invitrogen), CD49b (clone HMa2; BD), CD25 (clone PC61; eBioscience), CD69 (clone H1.2F3; BD), Foxp3 (clone FJK-16 s; eBioscience), IFNγ (clone XMG1.2; BD), TNF-α (clone MP6-XP22; BD), IL-2 (clone JES6-5H4; BD), IL-4 (clone 11B11; BD), IL-17 (clone TC11-18H10; BD), or IL-10 (clone JES5-16E3; BD). Foxp3 staining was performed according to the manufacturer's instructions (eBiosciences). For intracellular cytokine staining, cells were stimulated with PMA (50 ng/ml) (Sigma) and ionomycin (1 nM) (Calbiochem) for 4 hr. Golgistop (BD) was added to the culture in the recommended amount during the last 3 hr, followed by fixing and permeabilization according to the manufacturer's instructions (BD). In vivo NK cell cytotoxicity assay: Treg cells were depleted in BDC2.5/NOD.Foxp3^{DTR+} mice by DT 2 days before 1 × 10^7 CFSE-labeled target cell were i.v. injected. Target cells were a mix of splenocyte populations (CFSE^{lo} MHCI-negative targets [B2m-deficient NOD cells] and CFSE^{hi} MHCI-positive controls [WT NOD cells]); 16 hr later, NK-cell-kill activity was measured in different organs by comparing the ratio of the two populations in reference to the input mix.

For BrdU staining, BrdU (1 mg, Sigma) was i.v. injected 48 hr after DT administration, and the mice were sacrificed 1 hr later. The pancreas and PLN were removed and digested for about 15 min with collagenase type IV (1 mg/ml; Sigma) and DNase (0.5 mg/ml; Sigma). Cells were fixed and permeabilized according to the manufacturer's instructions (BD) for BrdU staining and were then analyzed using the LSRII instrument and FlowJo software.

Microarrays

RNA was prepared from sorted CD4$^+$ T cell populations from BDC2.5/NOD.Foxp3^{DTR+} mice using Trizol as described (Yamagata et al., 2004). RNA was amplified for two rounds (MessageAmp aRNA, Ambion), biotin-labeled (BioArray High Yield RNA Transcription Labeling, Enzo), and purified using the RNeasy Mini Kit (QIAGEN). The resulting cRNAs were hybridized to M430 2.0 chips (Affymetrix). All of the cell populations analyzed were generated in duplicate or triplicate. Raw data were normalized using the RMA algorithm

implemented in the "Expression File Creator" module from the GenePattern software package (Reich et al., 2006). Data were visualized using the "Multiplot" modules from GenePattern.

ACCESSION NUMBERS

Datasets have been deposited at NCBI-GEO under accession no. GSE18136.

SUPPLEMENTAL DATA

Supplemental Data include one table and four figures and can be found with this article online at http://www.cell.com/immunity/supplemental/S1074-7613(09)00411-7.

ACKNOWLEDGMENTS

We thank J. Stockton for producing the DTR transgenics; J. LaVecchio and G. Buruzala for flow cytometry; J. Hill, J. Perez, and K. Leatherbee for help with the microarray analyses; and H.-J. Wu for the IFN-γ signature. This work was supported by grants from the Juvenile Diabetes Research Foundation (4-2007-1057) and the NIH (R01 DK59658) to D.M. and C.B.; by grants from the Sandler Program in Asthma Research and the National Multiple Sclerosis Society to D.R.L.; and by the core facilities of Joslin Diabetes Center's NIDDK-funded Diabetes and Endocrinology Research Center. M.F. was supported by postdoctoral fellowships from the German Research Foundation (Emmy-Noether Fellowship, FE 801/1-1) and the Charles A. King Trust.

Received: November 13, 2008
Revised: July 27, 2009
Accepted: August 13, 2009
Published online: October 8, 2009

REFERENCES

Alba, A., Planas, R., Clemente, X., Carrillo, J., Ampudia, R., Puertas, M.C., Pastor, X., Tolosa, E., Pujol-Borrell, R., Verdaguer, J., et al. (2008). Natural killer cells are required for accelerated type 1 diabetes driven by interferon-beta. Clin. Exp. Immunol. *151*, 467–475.

Bennett, C.L., Christie, J., Ramsdell, F., Brunkow, M.E., Ferguson, P.J., Whitesell, L., Kelly, T.E., Saulsbury, F.T., Chance, P.F., and Ochs, H.D. (2001). The immune dysregulation, polyendocrinopathy, enteropathy, X-linked syndrome (IPEX) is caused by mutations of FOXP3. Nat. Genet. *27*, 20–21.

Bennett, C.L., and Clausen, B.E. (2007). DC ablation in mice: promises, pitfalls, and challenges. Trends Immunol. *28*, 525–531.

Bour-Jordan, H., Salomon, B.L., Thompson, H.L., Szot, G.L., Bernhard, M.R., and Bluestone, J.A. (2004). Costimulation controls diabetes by altering the balance of pathogenic and regulatory T cells. J. Clin. Invest. *114*, 979–987.

Carnaud, C., Gombert, J., Donnars, O., Garchon, H., and Herbelin, A. (2001). Protection against diabetes and improved NK/NKT cell performance in NOD.NK1.1 mice congenic at the NK complex. J. Immunol. *166*, 2404–2411.

Chen, Z., Herman, A.E., Matos, M., Mathis, D., and Benoist, C. (2005). Where CD4+CD25+ T reg cells impinge on autoimmune diabetes. J. Exp. Med. *202*, 1387–1397.

Debray-Sachs, M., Carnaud, C., Boitard, C., Cohen, H., Gresser, I., Bedossa, P., and Bach, J.-F. (1991). Prevention of diabetes in NOD mice treated with antibody to murine IFNγ. J. Autoimmun. *4*, 237–248.

Esensten, J.H., Lee, M.R., Glimcher, L.H., and Bluestone, J.A. (2009). T-bet-deficient NOD mice are protected from diabetes due to defects in both T Cell and innate immune system function. J. Immunol. *183*, 75–82.

Feuerer, M., Herrero, L., Cipolletta, D., Naaz, A., Wong, J., Nayer, A., Lee, J., Goldfine, A., Benoist, C., Shoelson, S.E., et al. (2009). Lean, but not obese, fat is enriched for a unique population of regulatory T cells that affect metabolic parameters. Nat. Med. *15*, 930–939.

Ghiringhelli, F., Menard, C., Terme, M., Flament, C., Taieb, J., Chaput, N., Puig, P.E., Novault, S., Escudier, B., Vivier, E., et al. (2005). CD4+CD25+ regulatory T cells inhibit natural killer cell functions in a transforming growth factor-beta-dependent manner. J. Exp. Med. *202*, 1075–1085.

Gonzalez, A., Katz, J.D., Mattei, M.G., Kikutani, H., Benoist, C., and Mathis, D. (1997). Genetic control of diabetes progression. Immunity *7*, 873–883.

Gregori, S., Giarratana, N., Smiroldo, S., and Adorini, L. (2003). Dynamics of pathogenic and suppressor T cells in autoimmune diabetes development. J. Immunol. *171*, 4040–4047.

Haskins, K., Portas, M., Bradley, B., Wegmann, D., and Lafferty, K.J. (1988). T-lymphocyte clone specific for pancreatic islet antigen. Diabetes *37*, 1444–1448.

Herman, A.E., Freeman, G.J., Mathis, D., and Benoist, C. (2004). CD4+CD25+ T regulatory cells dependent on ICOS promote regulation of effector cells in the prediabetic lesion. J. Exp. Med. *199*, 1479–1489.

Hill, J., Feuerer, M., Tash, K., Haxhinasto, S., Perez, J., Melamed, R., Mathis, D., and Benoist, C. (2007). Foxp3-dependent and independent regulation of the Treg transcriptional signature. Immunity *27*, 786–800.

Hultgren, B., Huang, X., Dybdal, N., and Stewart, T.A. (1996). Genetic absence of γ-interferon delays but does not prevent diabetes in NOD mice. Diabetes *45*, 812–817.

Kanagawa, O., Xu, G., Tevaarwerk, A., and Vaupel, B.A. (2000). Protection of nonobese diabetic mice from diabetes by gene(s) closely linked to IFN-gamma receptor loci. J. Immunol. *164*, 3919–3923.

Kanagawa, O., Militech, A., and Vaupel, B.A. (2002). Regulation of diabetes development by regulatory T cells in pancreatic islet antigen-specific TCR transgenic nonobese diabetic mice. J. Immunol. *168*, 6159–6164.

Katz, J.D., Wang, B., Haskins, K., Benoist, C., and Mathis, D. (1993). Following a diabetogenic T cell from genesis through pathogenesis. Cell *74*, 1089–1100.

Katz, J.D., Benoist, C., and Mathis, D. (1995). T helper cell subsets in insulin-dependent diabetes. Science *268*, 1185–1188.

Kim, J.M., Rasmussen, J.P., and Rudensky, A.Y. (2007). Regulatory T cells prevent catastrophic autoimmunity throughout the lifespan of mice. Nat. Immunol. *8*, 191–197.

Korn, T., Reddy, J., Gao, W., Bettelli, E., Awasthi, A., Petersen, T.R., Backstrom, B.T., Sobel, R.A., Wucherpfennig, K.W., Strom, T.B., et al. (2007). Myelin-specific regulatory T cells accumulate in the CNS but fail to control autoimmune inflammation. Nat. Med. *13*, 423–431.

Lahl, K., Loddenkemper, C., Drouin, C., Freyer, J., Arnason, J., Eberl, G., Hamann, A., Wagner, H., Huehn, J., and Sparwasser, T. (2007). Selective depletion of Foxp3+ regulatory T cells induces a scurfy-like disease. J. Exp. Med. *204*, 57–63.

Luhder, F., Höglund, P., Allison, J.P., Benoist, C., and Mathis, D. (1998). Cytotoxic T lymphocyte-associated antigen 4 regulates the unfolding of autoimmune diabetes. J. Exp. Med. *187*, 427–432.

Lund, J.M., Hsing, L., Pham, T.T., and Rudensky, A.Y. (2008). Coordination of early protective immunity to viral infection by regulatory T cells. Science *320*, 1220–1224.

Martin-Fontecha, A., Thomsen, L.L., Brett, S., Gerard, C., Lipp, M., Lanzavecchia, A., and Sallusto, F. (2004). Induced recruitment of NK cells to lymph nodes provides IFN-gamma for T(H)1 priming. Nat. Immunol. *5*, 1260–1265.

Poirot, L., Benoist, C., and Mathis, D. (2004). Natural killer cells distinguish innocuous and destructive forms of pancreatic islet autoimmunity. Proc. Natl. Acad. Sci. USA *101*, 8102–8107.

Reich, M., Liefeld, T., Gould, J., Lerner, J., Tamayo, P., and Mesirov, J.P. (2006). GenePattern 2.0. Nat. Genet. *38*, 500–501.

Saito, M., Iwawaki, T., Taya, C., Yonekawa, H., Noda, M., Inui, Y., Mekada, E., Kimata, Y., Tsuru, A., and Kohno, K. (2001). Diphtheria toxin receptor-mediated conditional and targeted cell ablation in transgenic mice. Nat. Biotechnol. *19*, 746–750.

Sakaguchi, S., Yamaguchi, T., Nomura, T., and Ono, M. (2008). Regulatory T cells and immune tolerance. Cell *133*, 775–787.

Salomon, B., Lenschow, D.J., Rhee, L., Ashourian, N., Singh, B., Sharpe, A., and Bluestone, J.A. (2000). B7/CD28 costimulation is essential for the

homeostasis of the CD4+CD25+ immunoregulatory T cells that control autoimmune diabetes. Immunity *12*, 431–440.

Sarween, N., Chodos, A., Raykundalia, C., Khan, M., Abbas, A.K., and Walker, L.S. (2004). CD4+CD25+ cells controlling a pathogenic CD4 response inhibit cytokine differentiation. CXCR-3 expression, and tissue invasion. J. Immunol. *173*, 2942–2951.

Serreze, D.V., Post, C.M., Chapman, H.D., Johnson, E.A., Lu, B., and Rothman, P.B. (2000). Interferon-gamma receptor signaling is dispensable in the development of autoimmune type 1 diabetes in NOD mice. Diabetes *49*, 2007–2011.

Tang, Q., and Bluestone, J.A. (2008). The Foxp3+ regulatory T cell: a jack of all trades, master of regulation. Nat. Immunol. *9*, 239–244.

Tang, Q., Henriksen, K.J., Bi, M., Finger, E.B., Szot, G., Ye, J., Masteller, E.L., McDevitt, H., Bonyhadi, M., and Bluestone, J.A. (2004). In Vitro-expanded Antigen-specific Regulatory T Cells Suppress Autoimmune Diabetes. J. Exp. Med. *199*, 1455–1465.

Tang, Q., Adams, J.Y., Tooley, A.J., Bi, M., Fife, B.T., Serra, P., Santamaria, P., Locksley, R.M., Krummel, M.F., and Bluestone, J.A. (2006). Visualizing regulatory T cell control of autoimmune responses in nonobese diabetic mice. Nat. Immunol. *7*, 83–92.

Tarbell, K.V., Yamazaki, S., Olson, K., Toy, P., and Steinman, R.M. (2004). CD25+ CD4+ T Cells, Expanded with Dendritic Cells Presenting a Single Autoantigenic Peptide, Suppress Autoimmune Diabetes. J. Exp. Med. *199*, 1467–1477.

Tarbell, K.V., Petit, L., Zuo, X., Toy, P., Luo, X., Mqadmi, A., Yang, H., Suthanthiran, M., Mojsov, S., and Steinman, R.M. (2007). Dendritic cell-expanded, islet-specific CD4+ CD25+ CD62L+ regulatory T cells restore normoglycemia in diabetic NOD mice. J. Exp. Med. *204*, 191–201.

Terme, M., Chaput, N., Combadiere, B., Ma, A., Ohteki, T., and Zitvogel, L. (2008). Regulatory T cells control dendritic cell/NK cell cross-talk in lymph nodes at the steady state by inhibiting CD4+ self-reactive T cells. J. Immunol. *180*, 4679–4686.

Tritt, M., Sgouroudis, E., d'Hennezel, E., Albanese, A., and Piccirillo, C.A. (2008). Functional waning of naturally occurring CD4+ regulatory T-cells contributes to the onset of autoimmune diabetes. Diabetes *57*, 113–123.

Wildin, R.S., Ramsdell, F., Peake, J., Faravelli, F., Casanova, J.L., Buist, N., Levy-Lahad, E., Mazzella, M., Goulet, O., Perroni, L., et al. (2001). X-linked neonatal diabetes mellitus, enteropathy and endocrinopathy syndrome is the human equivalent of mouse scurfy. Nat. Genet. *27*, 18–20.

Wu, H.J., Sawaya, H., Binstadt, B., Brickelmaier, M., Blasius, A., Gorelik, L., Mahmood, U., Weissleder, R., Carulli, J., Benoist, C., et al. (2007). Inflammatory arthritis can be reined in by CpG-induced DC-NK cell cross talk. J. Exp. Med. *204*, 1911–1922.

Yamagata, T., Mathis, D., and Benoist, C. (2004). Self-reactivity in thymic double-positive cells commits cells to a CD8 alpha alpha lineage with characteristics of innate immune cells. Nat. Immunol. *5*, 597–605.

You, S., Belghith, M., Cobbold, S., Alyanakian, M.A., Gouarin, C., Barriot, S., Garcia, C., Waldmann, H., Bach, J.F., and Chatenoud, L. (2005). Autoimmune diabetes onset results from qualitative rather than quantitative age-dependent changes in pathogenic T-cells. Diabetes *54*, 1415–1422.

Zheng, Y., and Rudensky, A.Y. (2007). Foxp3 in control of the regulatory T cell lineage. Nat. Immunol. *8*, 457–462.